Effect of Running Speed on Lower Limb Joint Kinetics

ANTHONY G. SCHACHE[1], PETER D. BLANCH[2], TIM W. DORN[1], NICHOLAS A. T. BROWN[3], DOUG ROSEMOND[3], and MARCUS G. PANDY[1]

[1]*Department of Mechanical Engineering, University of Melbourne, Victoria, AUSTRALIA;* [2]*Department of Physical Therapies, Australian Institute of Sport, Belconnen, ACT, AUSTRALIA; and* [3]*Department of Biomechanics and Performance Analysis, Australian Institute of Sport, Belconnen, ACT, AUSTRALIA*

ABSTRACT

SCHACHE, A. G., P. D. BLANCH, T. W. DORN, N. A. T. BROWN, D. ROSEMOND, and M. G. PANDY. Effect of Running Speed on Lower Limb Joint Kinetics. *Med. Sci. Sports Exerc.*, Vol. 43, No. 7, pp. 1260–1271, 2011. **Purpose**: Knowledge regarding the biomechanical function of the lower limb muscle groups across a range of running speeds is important in improving the existing understanding of human high performance as well as in aiding in the identification of factors that might be related to injury. The purpose of this study was to evaluate the effect of running speed on lower limb joint kinetics. **Methods**: Kinematic and ground reaction force data were collected from eight participants (five males and three females) during steady-state running on an indoor synthetic track at four discrete speeds: 3.50 ± 0.04, 5.02 ± 0.10, 6.97 ± 0.09, and 8.95 ± 0.70 $m \cdot s^{-1}$. A standard inverse-dynamics approach was used to compute three-dimensional torques at the hip, knee, and ankle joints, from which net powers and work were also calculated. A total of 33 torque, power, and work variables were extracted from the data set, and their magnitudes were statistically analyzed for significant speed effects. **Results**: The torques developed about the lower limb joints during running displayed identifiable profiles in all three anatomical planes. The sagittal-plane torques, net powers, and work done at the hip and knee during terminal swing demonstrated the largest increases in absolute magnitude with faster running. In contrast, the work done at the knee joint during stance was unaffected by increasing running speed, whereas the work done at the ankle joint during stance increased when running speed changed from 3.50 to 5.02 $m \cdot s^{-1}$, but it appeared to plateau thereafter. **Conclusions**: Of all the major lower limb muscle groups, the hip extensor and knee flexor muscles during terminal swing demonstrated the most dramatic increase in biomechanical load when running speed progressed toward maximal sprinting. **Key Words:** GAIT BIOMECHANICS, INVERSE DYNAMICS, JOINT TORQUE, JOINT POWER, HAMSTRING MUSCLE

Knowledge regarding the biomechanical function of the lower limb muscle groups across a range of running speeds is important in improving existing understanding of human high performance as well as in aiding in the identification of factors that might be related to injury. A common approach for quantifying the biomechanical function of lower limb muscle groups during running is inverse dynamics, which is the process of determining the lower limb joint moments of force (or torques) on the basis of measured joint kinematics, ground reaction forces, and segmental inertial properties (38). The primary parameters of interest include (a) torques, (b) net powers (product of the torque and angular velocity about a joint), and (c) work (area under the net power vs time curve). When interpreted together, these parameters provide insight into the biomechanical causes of the observed movement pattern; more specifically, whether lower limb muscle groups are acting concentrically and generating energy or are acting eccentrically and absorbing energy.

Many studies have computed torques, net powers, and/or work done at the lower limb joints during running (1,3,5,7–9,12,16,20,23,30,33,37,40) and sprinting (5,6,13,19–22,29,34). Although these studies have provided much insight into the biomechanical function of the lower limb muscle groups across a range of running speeds for adult humans, they are not without limitations. First, most studies have evaluated only certain phases of the stride cycle; specifically, either the stance (3,5–8,12,16,21,23,30) or swing phase (9,13,33,34). Second, many studies have either obtained data for a single speed (6,8,12,13,16,19,21,22,29,34,37) or have obtained data across a range of speeds but have not included maximal sprinting (3,7,30,33,40). Third, almost all studies have used a two-dimensional approach focusing exclusively on sagittal-plane dynamics (1,3,5–9,12,13,19–22,29,30,33,34,37,40). However, an understanding of non–sagittal-plane dynamics is also likely to be important. Both Glitsch and Baumann (16)

Address for correspondence: Anthony G. Schache, Ph.D., Department of Mechanical Engineering, The University of Melbourne, Victoria 3010, Australia; E-mail: anthonys@unimelb.edu.au.
Submitted for publication June 2010.
Accepted for publication November 2010.

Supplemental digital content is available for this article. Direct URL citations appear in the printed text and are provided in the HTML and PDF versions of this article on the journal's Web site (www.acsm-msse.org).

0195-9131/11/4307-1260/0
MEDICINE & SCIENCE IN SPORTS & EXERCISE®

DOI: 10.1249/MSS.0b013e3182084929

and McClay and Manal (23) demonstrated that, during an almost planar movement such as running, the lower limb joints are associated with significant three-dimensional torques, especially in the frontal plane. Furthermore, Stefanyshyn et al. (32) found a relationship between frontal-plane knee joint dynamics during running and risk of injury. Although these studies highlight the potential importance of non–sagittal-plane dynamics during running, data from both Glitsch and Baumann (16) and McClay and Manal (23) are limited to the stance phase of the stride cycle and a single speed of running only. In view of these limitations, further research is needed to generate a more complete analysis regarding the effects of increasing running speed on lower limb joint kinetics.

Many lower limb muscles that play an important role during running have specific actions that are not limited to a single anatomical plane. For example, in addition to being a strong hip extensor, the gluteus maximus muscle also has a large capacity for producing hip external rotation (11,26). Similarly, the rectus femoris and biceps femoris muscles have been shown to be capable of inducing both sagittal- and frontal-plane hip motion (18). Consequently, running is likely to be fundamentally governed by coordinated synchronous muscle activity in all three anatomical planes, which would suggest that any investigation into the biomechanics of running ideally should be approached from a three-dimensional perspective.

The aim of the current study was twofold: first, to use an inverse-dynamics approach to quantify the three-dimensional torques at the lower limb joints across the entire stride cycle during overground running; and second, to determine the effect of increasing running speed on the magnitude of the torques, net powers, and work done at the lower limb joints.

METHODS

Participants. Eight participants (five males and three females) were recruited from running-based sports, such as track and field ($n = 7$) and Australian Rules football ($n = 1$). Participants had a mean ± SD age of 27.0 ± 7.8 yr, a mean ± SD height of 176.2 ± 8.1 cm, and a mean ± SD body mass of 73.0 ± 8.6 kg. At the time of testing, all participants had been free from any musculoskeletal injury likely to adversely affect their running mechanics for at least a 6-month period. The study was approved by the Human Research Ethics Committee at The University of Melbourne and The Australian Institute of Sport, and all participants gave their written informed consent before testing.

Instrumentation. All testing took place on an indoor 110-m synthetic running track in the Biomechanics Laboratory at the Australian Institute of Sport. Kinematic data were acquired using a three-dimensional motion analysis system (VICON; Oxford Metrics Ltd., Oxford, United Kingdom) with 22 cameras sampling at a rate of 250 Hz. The measurement volume had a length, width, and height of 15, 1.3, and 2.2 m, respectively, and was situated approximately 80 m along the 110-m running track allowing ample distance for acceleration and deceleration. The calibration error for the measurement volume was estimated to be no greater than 1 mm for all cameras. Eight large (900 × 600-mm^2) Kistler force plates (Kistler Instrument Corp., Amherst, NY) sampling at a rate of 1500 Hz were used to capture ground reaction force data. All force plates were embedded in the floor of the laboratory and were covered with a piece of the synthetic running track to disguise their location to the participants, thus preventing any force plate targeting. The eight force plates were situated immediately adjacent to each other (thereby expanding a total length of 7.2 m) and were located at the center of the calibrated measurement volume.

Procedures. A four-segment, hierarchical, biomechanical model (pelvis, left thigh, left shank, and left foot) was used in this study. Each lower limb joint (hip, knee, and ankle) was modeled as a ball-and-socket joint described by three angles. To define the model, small reflective markers were mounted on each participant's pelvis and left lower limb (see Figure, Supplemental Digital Content 1, Marker setup for experimental data collection, http://links.lww.com/MSS/A80). Specifically, an elastic strap (~4 cm wide) was tightly secured around the pelvis. A light thermoplastic triangular plate containing four reflective markers (i.e., three markers positioned along the superior border and one marker positioned at the inferior apex) was attached to the back of the strap. The strap was placed on the pelvis such that the triangular plate was mounted on the sacrum with the middle superior marker overlying the midpoint between the two posterior superior iliac spines. A 10-cm-long thermoplastic bar, which contained two markers fixed to either end, was mounted on the lateral aspect of the thigh. Single markers were affixed to the anterior and distal aspects of the thigh, both the superior and inferior aspects of the anteromedial shaft of the tibia, the mid and lateral aspects of the shank, the inferoposterior aspect of the heel, as well as the medial and lateral midfoot. To establish joint centers and define segmental anatomical coordinate systems, additional "calibration" markers were also affixed to the following locations: left and right anterior superior iliac spines, medial and lateral femoral condyles, medial and lateral malleoli, the superoposterior aspect of the heel, and on the forefoot at the junction between the second and third metatarsophalangeal joints.

For testing, the participants wore standard athletic shorts and running sandals (NIKE Straprunner IV Beaverton, Oregon) that allowed adequate exposure of the foot for marker placement (see Figure, Supplemental Digital Content 1, Marker setup for experimental data collection, http://links.lww.com/MSS/A80). Data collection commenced with the recording of several anthropometric parameters, which included height, body mass, and pelvic width. Markers were then placed on each participant's pelvis and left lower limb as described above. A static trial was collected with the participant standing in the anatomical position, after which the "calibration" markers were removed. A dynamic calibration trial was then collected. The participant stood on his/her right lower limb and performed three continuous isolated flexion–extension motions of the left

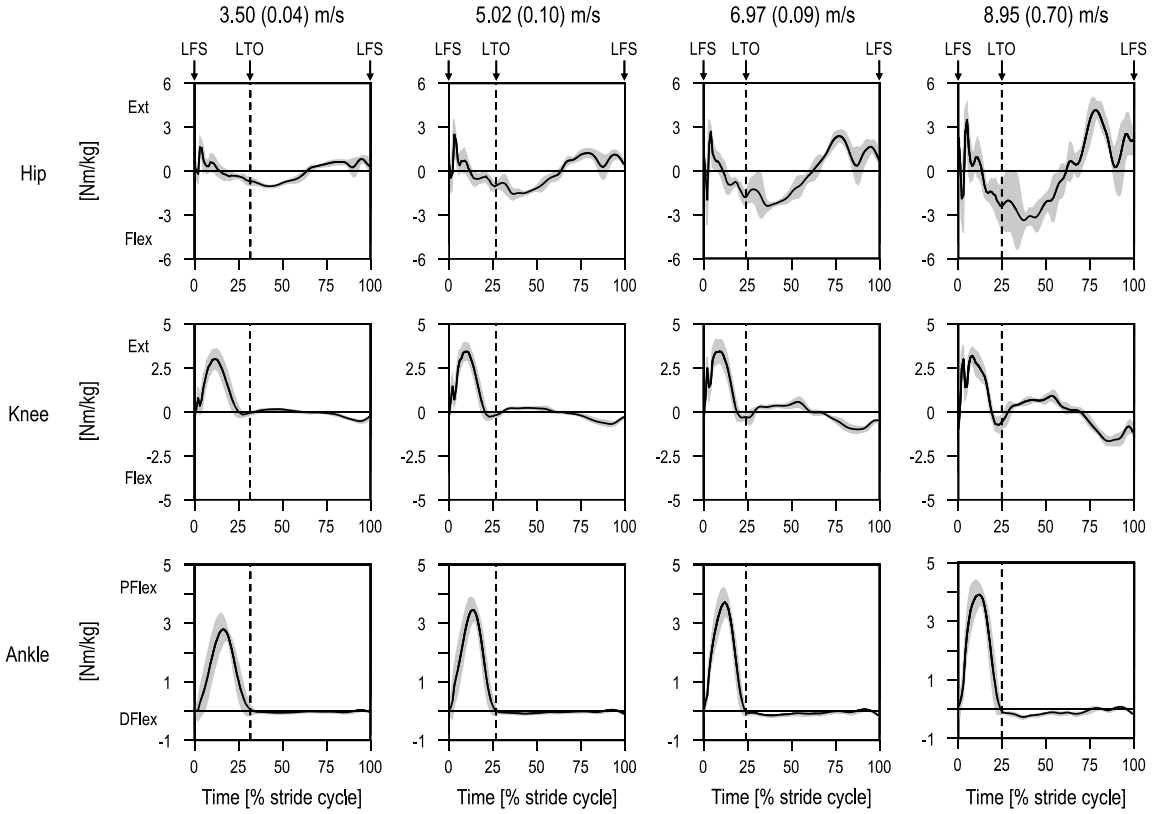

FIGURE 1—Sagittal-plane torques developed about the hip (*top panels*), knee (*middle panels*), and ankle (*bottom panels*) joints across the full stride cycle for the left lower limb (left foot strike to left foot strike) for the four discrete running speeds. Data represent the group mean (*solid black line*) ± one SD (*gray shading*). The running speeds of 3.50, 5.02, and 6.97 $m \cdot s^{-1}$ contain data for eight subjects, whereas the running speed of 8.97 $m \cdot s^{-1}$ contains data for seven subjects. The *dashed vertical line* indicates the average time (% stride cycle) of toe-off for each speed condition. Ext, extension; Flex, flexion; PFlex, plantarflexion; DFlex, dorsiflexion; LFS, left foot strike; LTO, left toe-off.

knee through a range of 0° to 90°. The participant was required to keep the left thigh as stationary as possible throughout the duration of the motion so as to minimize thigh-marker soft tissue artifact as much as possible.

Before commencing the running trials, all participants completed a warm-up consisting of repeated walking and slow jogging trials to familiarize themselves with the experimental conditions. Data were collected at the following running speeds: 3.5, 5.0, and 7.0 $m \cdot s^{-1}$ and maximum sprinting. For practical reasons, the order of running speeds was incremental rather than randomized. The slower speeds of running provided a graduated warm-up before performing the maximum sprinting trials. For each trial, participants were instructed to maintain a steady-state speed throughout the calibrated measurement volume. There were no restrictions placed on acceleration and deceleration distances. Running speed was recorded using timing gates (Speedlight Telemetry Timing; Swift Performance Equipment, Walcol, Australia) positioned 20 m apart at each end of the calibrated measurement volume. Participants were provided with feedback after each running trial to reproduce the desired running speeds. For the prescribed speed conditions, participants performed repeated trials until a single trial was obtained whereby the measured speed was within ±5% of the desired speed. Adequate recovery time was provided between speed increments so as to avoid the effects of fatigue. Seven participants completed all running speed conditions, whereas one participant did not complete the maximum sprinting condition.

Data analysis. Marker trajectories were filtered using Woltring's (39) general cross-validatory quintic smoothing spline with a predicted mean squared error of 15 mm. Both the static and dynamic calibration trials were used to reconstruct the anatomical coordinate systems for each body segment in the hierarchical biomechanical model. The hip joint center was defined using the approach described by Harrington et al. (17) and was reconstructed relative to the pelvic tracking markers (triangular sacral plate) in the dynamic trials. The knee joint center was defined as the midpoint between the medial and lateral femoral condyle markers and was reconstructed relative to the shank tracking markers in the dynamic trials. The dynamic calibration task (i.e., an open-chain isolated knee flexion–extension motion) was used to determine the orientation of the mediolateral axis of the femoral anatomical coordinate system (or knee joint flexion–extension axis) based on a previously described numerical approach (28). The ankle joint center was defined as the midpoint between the medial and lateral malleoli markers and was reconstructed relative to the shank tracking

markers in the dynamic trials. Full details regarding the anatomical coordinate systems for each body segment can be found elsewhere (27).

Only trials containing a valid foot strike for the left leg (i.e., foot strike occurred well within the boundaries of a single force plate) were analyzed. In the instance that a given trial contained more than one valid foot strike on a force plate for the left leg (e.g., as occurred for the slower running speeds), then the stride cycle closest to the center of the calibrated measurement volume was chosen. A standard inverse-dynamics approach was used to calculate the internal torques developed by the lower limb joints (38). Segmental inertial parameters were taken from de Leva (10). Ground reaction force data were not filtered during the inverse-dynamics process. The center of pressure location and vertical free torque were calculated using the ground reaction forces, torques, and calibration measurements from the relevant force plate. Ground reaction forces and the vertical free torque were then applied directly to the foot segment at the center of pressure location, and three-dimensional joint torques were calculated from the ground up (38). All torques were expressed in a nonorthogonal reference frame or joint coordinate system (27). For each joint, power was calculated as the product of the net torque and angular velocity. Because power is a scalar quantity, only the net power at each lower limb joint was computed. The amount of positive and negative work done at the hip, knee, and ankle joints at distinct phases throughout the stride cycle was calculated by integrating the relevant portion of the power-versus-time curve (i.e., area under the curve) (37). All torque, power, and work data for each participant were normalized by dividing by body mass. Bodybuilder software (VICON; Oxford Metrics Ltd.) was used to perform all computations.

Discrete torque, power, and work variables were extracted from the data set for statistical analysis. Various maxima and minima points that were readily identifiable on the torque and power profiles at the hip, knee, and ankle joints for each participant at each running speed were chosen for analysis. Also, 10 distinct phases in the stride cycle, where it was evident that continuous positive or negative work was being done at the lower limb joints for all running speeds, were identified and chosen for analysis (see Figure, Supplemental Digital Content 2, the 10 distinct periods of continuous positive or negative work done at the lower limb joints identified across the stride cycle for all running speeds, http://links.lww.com/MSS/A81). (see Figure, Supplemental Digital Content 1, Marker setup for experimental data collection, http://links.lww.com/MSS/A80). A total of 33 torque, power, and work variables were statistically analyzed. One-way repeated-measures ANOVA tests were used to determine which of the dependent variables were significantly affected by running speed. When significant F ratios were obtained, *post hoc* pairwise comparisons (paired t-test) were used to determine differences between each of the running speeds. A conservative level of significance was set at $P < 0.008$ for all tests, which was determined by applying a Bonferroni correction to a significance level of $P < 0.05$ (i.e., a total of six *post hoc* pairwise comparisons were performed per dependent variable). To generate a complete data set for purposes of statistical analyses, data for one participant for the maximum sprinting speed were imputed using a mean substitution (15). For each dependent variable, data for this participant were assumed to equal the mean of the sample of available data ($n = 7$) for the maximum sprinting condition. This approach was considered reasonable given that, for each ANOVA, the extent of missing data was small (i.e., limited to a single-speed condition for one participant only). The statistical association between running speed and work done at the lower limb joints was also computed. Second-order polynomial trend lines were fitted to the data for all work variables that were identified from the data set and corresponding coefficient of determination (R^2) values were calculated. Linear trend lines were explored, but they yielded lower R^2 values.

RESULTS

The mean ± SD running speeds were 3.50 ± 0.04, 5.02 ± 0.10, 6.97 ± 0.09, and 8.95 ± 0.70 $m \cdot s^{-1}$. The mean ± SD magnitudes for the various discrete variables extracted from the data, as well as the results from statistical testing, are displayed in Table 1. Overall, a significant speed effect ($P < 0.008$) was observed for 29 of the 33 variables, with the absolute magnitude of these 29 variables increasing with faster running. *Post hoc* tests revealed that not all running speed conditions were significantly different from each other. Only 12 of the 29 variables were found to display significant increases in absolute magnitude for all running speed increments (variables indicated with gray shading in Table 1). All of these 12 variables related specifically to the biomechanical function of the hip and knee joints during swing.

The normalized mean ± SD sagittal-plane torques developed about the hip, knee, and ankle joints across the full stride cycle for each running speed condition are presented in Figure 1. At the hip joint, a flexion torque developed for a short period immediately after foot strike, which was a consequence of the rapid increase in magnitude of the fore-aft component of the ground reaction force. An extension torque then developed about the hip during the first half of stance before becoming flexion again during the latter half of stance. The hip flexion torque continued during the first half of swing. Finally, a hip extension torque developed during the last half of swing. At the knee joint, an extension torque occurred for the majority of stance, which was followed by a small flexion torque just before toe-off. A knee extension torque then developed again during the first half of swing, whereas a knee flexion torque developed during the first half of swing, whereas a knee flexor torque developed during the last half of swing. At the ankle joint, a large plantarflexion torque occurred during stance, which peaked around midstance and decreased by toe-off. The torque at the ankle joint during swing was minimal. As running speed increased, the characteristic profiles of the sagittal-plane

TABLE 1. Mean ± SD magnitudes for the torque, power and work variables.

Variable	Speed 1 (n = 8) 3.50 ± 0.04 m·s^{-1}	Speed 2 (n = 8) 5.02 ± 0.10 m·s^{-1}	Speed 3 (n = 8) 6.97 ± 0.09 m·s^{-1}	Speed 4 (n = 7) 8.95 ± 0.70 m·s^{-1}	Effect Size (Partial η^2)
Hip					
$T_{\text{Peak extension initial stance}}$ (N·m·kg^{-1})*	2.02 ± 0.36[3,4]	2.95 ± 1.08	3.18 ± 0.85[1]	4.09 ± 0.69[1]	0.68
$T_{\text{Peak flexion initial swing}}$ (N·m·kg^{-1})*	−1.09 ± 0.06[2,3,4]	−1.69 ± 0.25[1,3,4]	−2.59 ± 0.35[1,2,4]	−4.30 ± 0.87[1,2,3]	0.92
$T_{\text{Peak extension terminal swing}}$ (N·m·kg^{-1})*	0.91 ± 0.17[2,3,4]	1.41 ± 0.22[1,3,4]	2.45 ± 0.46[1,2,4]	4.18 ± 1.26[1,2,3]	0.89
$T_{\text{Peak abduction stance}}$ (N·m·kg^{-1})*	2.00 ± 0.26[3]	2.42 ± 0.80	3.10 ± 0.65[1]	3.29 ± 1.10	0.50
$T_{\text{Peak internal rotation stance}}$ (N·m·kg^{-1})*	0.49 ± 0.17[4]	0.56 ± 0.20	0.70 ± 0.28	0.99 ± 0.54[1]	0.59
$P_{\text{Peak absorption terminal stance}}$ (W·kg^{-1})*	−2.15 ± 0.83[2,3,4]	−5.56 ± 2.25[1,4]	−11.83 ± 5.29[1,4]	−22.93 ± 9.76[1,2,3]	0.81
$P_{\text{Peak generation initial swing}}$ (W·kg^{-1})*	3.80 ± 0.95[2,3,4]	7.55 ± 1.63[1,3,4]	15.16 ± 3.45[1,2,4]	29.01 ± 13.06[1,2,3]	0.81
$P_{\text{Peak absorption midswing}}$ (W·kg^{-1})*	−1.77 ± 0.88[2,3,4]	−3.98 ± 1.29[1,4]	−7.05 ± 2.75[1]	−23.45 ± 15.06[1,2]	0.68
$P_{\text{Peak generation terminal swing}}$ (W·kg^{-1})*	3.40 ± 0.95[2,3,4]	7.46 ± 3.06[1,3,4]	17.41 ± 5.39[1,2,4]	41.06 ± 9.42[1,2,3]	0.94
$W_{\text{Negative work done terminal stance}}$ (J·kg^{-1})*	−0.16 ± 0.13[3,4]	−0.23 ± 0.14[4]	−0.46 ± 0.22[1]	−0.69 ± 0.26[1,2]	0.78
$W_{\text{Positive work done initial swing}}$ (J·kg^{-1})*	0.42 ± 0.11[2,3,4]	0.74 ± 0.18[1,3,4]	1.10 ± 0.23[1,2,4]	1.67 ± 0.52[1,2,3]	0.87
$W_{\text{Negative work done midswing}}$ (J·kg^{-1})*	−0.10 ± 0.05[2,3,4]	−0.19 ± 0.08[1,3,4]	−0.38 ± 0.14[1,2]	−0.89 ± 0.47[1,2]	0.71
$W_{\text{Positive work done terminal swing}}$ (J·kg^{-1})*	0.31 ± 0.10[2,3,4]	0.65 ± 0.27[1,3,4]	1.22 ± 0.28[1,2,4]	2.28 ± 0.71[1,2,3]	0.91
Knee					
$T_{\text{Peak extension midstance}}$ (N·m·kg^{-1})	3.12 ± 0.56	3.52 ± 0.51	3.59 ± 0.63	3.55 ± 0.38	0.29
$T_{\text{Peak extension initial swing}}$ (N·m·kg^{-1})*	0.17 ± 0.02[2,3,4]	0.30 ± 0.07[1,3,4]	0.64 ± 0.24[1,2,4]	1.01 ± 0.26[1,2,3]	0.88
$T_{\text{Peak flexion terminal swing}}$ (N·m·kg^{-1})*	−0.53 ± 0.09[2,3,4]	−0.71 ± 0.13[1,3,4]	−1.08 ± 0.16[1,2,4]	−1.76 ± 0.28[1,2,3]	0.96
$T_{\text{Peak abduction stance}}$ (N·m·kg^{-1})*	0.65 ± 0.30[4]	0.99 ± 0.49	1.54 ± 0.59	1.42 ± 0.39[1]	0.50
$T_{\text{Peak external rotation stance}}$ (N·m·kg^{-1})*	−0.20 ± 0.08[3,4]	−0.32 ± 0.09	−0.30 ± 0.11[1]	−0.43 ± 0.11[1]	0.51
$P_{\text{Peak absorption initial stance}}$ (W·kg^{-1})*	−15.69 ± 4.80[3]	−18.67 ± 6.55[3]	−26.73 ± 7.72[1,2]	−28.70 ± 9.61	0.53
$P_{\text{Peak generation terminal stance}}$ (W·kg^{-1})*	7.72 ± 1.93[3,4]	11.04 ± 3.06	13.03 ± 3.26[1]	15.91 ± 5.06[1]	0.58
$P_{\text{Peak absorption initial swing}}$ (W·kg^{-1})*	−1.67 ± 0.34[2,3,4]	−3.21 ± 0.97[1,3,4]	−7.15 ± 2.48[1,2,4]	−13.95 ± 3.00[1,2,3]	0.92
$P_{\text{Peak absorption terminal swing}}$ (W·kg^{-1})*	−4.61 ± 0.61[2,3,4]	−8.50 ± 2.22[1,3,4]	−18.30 ± 3.59[1,2,4]	−37.15 ± 7.20[1,2,3]	0.95
$W_{\text{Negative work done initial stance}}$ (J·kg^{-1})	−0.74 ± 0.26	−0.78 ± 0.28	−0.83 ± 0.28	−0.60 ± 0.24	0.32
$W_{\text{Positive work done terminal stance}}$ (J·kg^{-1})	0.41 ± 0.13	0.44 ± 0.13	0.39 ± 0.16	0.34 ± 0.10	0.21
$W_{\text{Negative work done initial swing}}$ (J·kg^{-1})*	−0.19 ± 0.04[2,3,4]	−0.39 ± 0.10[1,3,4]	−0.71 ± 0.17[1,2,4]	−1.21 ± 0.26[1,2,3]	0.93
$W_{\text{Negative work done terminal swing}}$ (J·kg^{-1})*	−0.41 ± 0.04[2,3,4]	−0.77 ± 0.16[1,3,4]	−1.31 ± 0.23[1,2,4]	−2.07 ± 0.27[1,2,3]	0.97
Ankle					
$T_{\text{Peak plantarflexion midstance}}$ (N·m·kg^{-1})*	2.94 ± 0.35[2,3,4]	3.55 ± 0.39[1]	3.77 ± 0.44[1]	4.00 ± 0.42[1]	0.74
$T_{\text{Peak inversion stance}}$ (N·m·kg^{-1})*	0.24 ± 0.12[3,4]	0.31 ± 0.17	0.61 ± 0.20[1]	0.63 ± 0.15[1]	0.63
$T_{\text{Peak external rotation stance}}$ (N·m·kg^{-1})	−0.25 ± 0.11	−0.31 ± 0.05	−0.32 ± 0.08	−0.38 ± 0.13	0.32
$P_{\text{Peak absorption initial stance}}$ (W·kg^{-1})*	−7.77 ± 2.60[2,3,4]	−14.42 ± 3.81[1,3,4]	−23.79 ± 6.39[1,2]	−34.20 ± 13.27[1,2]	0.82
$P_{\text{Peak generation terminal stance}}$ (W·kg^{-1})*	16.09 ± 2.09[2,3,4]	27.25 ± 4.99[1,3,4]	37.10 ± 6.55[1,2]	46.98 ± 9.50[1,2]	0.89
$W_{\text{Negative work done initial stance}}$ (J·kg^{-1})*	−0.46 ± 0.16[2,3,4]	−0.69 ± 0.19[1]	−0.85 ± 0.18[1]	−0.83 ± 0.21[1]	0.65
$W_{\text{Positive work done terminal stance}}$ (J·kg^{-1})*	1.00 ± 0.10[2,3,4]	1.30 ± 0.19[1]	1.38 ± 0.20[1]	1.44 ± 0.21[1]	0.69

Gray shaded rows indicate variables that displayed significant increases in absolute magnitude for all running speed increments.
* Significant speed effect ($P < 0.008$).
[1] Significantly different from running speed 1 ($P < 0.008$).
[2] Significantly different from running speed 2 ($P < 0.008$).
[3] Significantly different from running speed 3 ($P < 0.008$).
[4] Significantly different from running speed 4 ($P < 0.008$).
η^2, eta-squared; P, power; T, torque; W, work.

torques remained consistent (Fig. 1). However, the maxima and minima points on the curves increased in absolute magnitude (Table 1). Of the seven variables extracted from the sagittal-plane torques, only peak knee extension torque during midstance was not found to display a significant speed effect. A significant increase in absolute magnitude for all running speed increments was shown by four variables: peak hip flexion torque during initial swing, peak hip extension torque during terminal swing, peak knee extension torque during initial swing, and peak knee flexion torque during terminal swing. When running speed changed from 3.50 to 8.95 m·s^{-1}, these variables increased in absolute magnitude by 3.21 N·m·kg^{-1} (3.94-fold), 3.27 N·m·kg^{-1} (4.59-fold), 0.84 N·m·kg^{-1} (5.94-fold), and 1.23 N·m·kg^{-1} (3.32-fold), respectively.

The normalized mean ± SD frontal-plane torques developed about the hip, knee, and ankle joints across the full stride cycle for each running speed condition are presented in Figure 2. At the hip joint, an abduction torque rapidly developed after foot strike that persisted for the majority of stance, after which an adduction torque developed just before toe-off. During swing, the frontal-plane torque at the hip fluctuated between small adduction and abduction torques. An adduction torque occurred during the final stages of swing, which continued through to the instant of foot strike. At the knee joint, an abduction torque developed during the first half of stance. For slower running speeds (3.50 and 5.02 m·s^{-1}), an abduction torque persisted until toe-off, but for faster running speeds (6.97 and 8.95 m·s^{-1}), an adduction torque developed at midstance and at toe-off. The frontal-plane torque at the knee joint was minimal for most of swing before a small abduction torque occurred just before foot strike. At the ankle joint, an inversion torque developed throughout initial and midstance, after which a

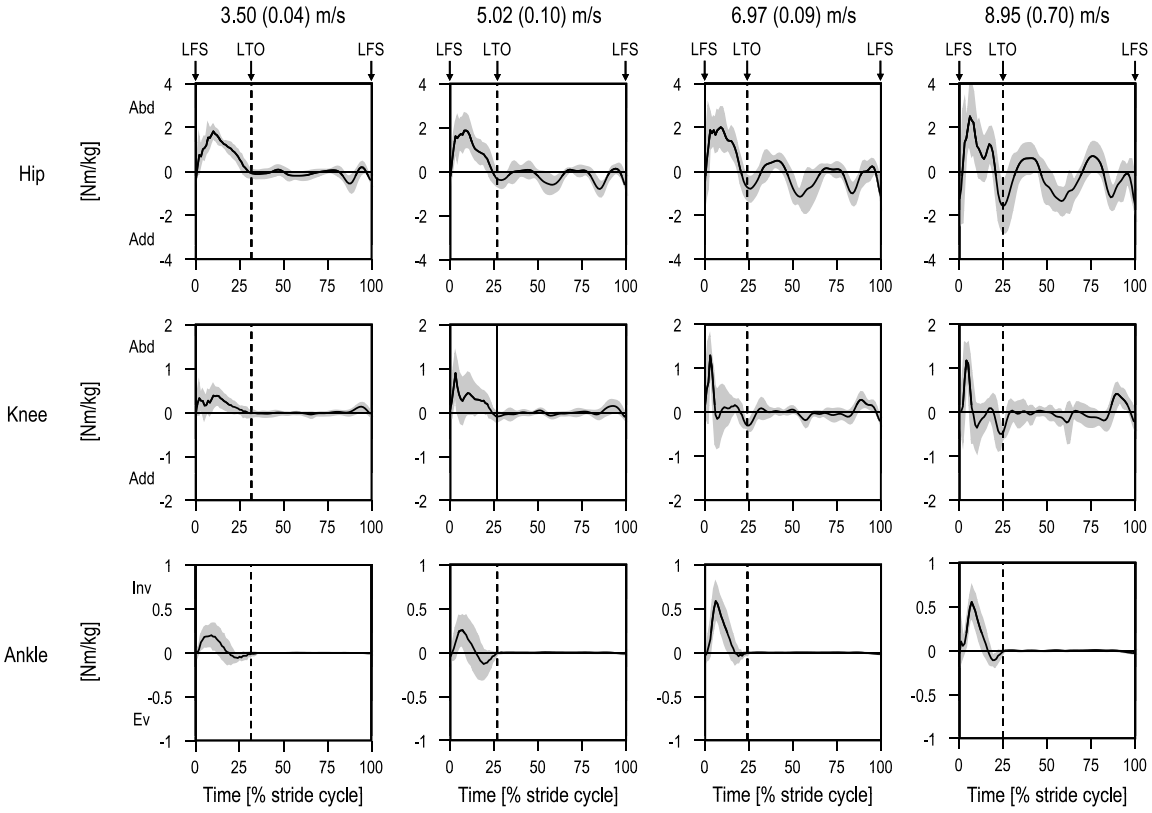

FIGURE 2—Frontal-plane torques developed about the hip (*top panels*), knee (*middle panels*), and ankle (*bottom panels*) joints across the full stride cycle for the left lower limb (left foot strike to left foot strike) for the four discrete running speeds. Data represent the group mean (*solid black line*) ± one SD (*gray shading*). The *dashed vertical line* indicates the average time (% stride cycle) of toe-off for each speed condition. LFS: left foot-strike; LTO: left toe-off; Abd, abduction; Add, adduction; Ev, eversion; Inv, inversion.

small eversion torque developed during terminal stance. The peak magnitudes of the frontal-plane torques during stance all displayed a significant speed effect (Table 1). Peak hip abduction torque during stance, peak knee abduction torque during stance, and peak ankle inversion torque during stance increased by 1.29 $N \cdot m \cdot kg^{-1}$ (1.65-fold), 0.77 $N \cdot m \cdot kg^{-1}$ (2.18-fold) and 0.39 $N \cdot m \cdot kg^{-1}$ (2.63-fold), respectively, when running speed changed from 3.50 to 8.95 $m \cdot s^{-1}$.

The normalized mean T SD transverse-plane torques developed the hip, knee, and ankle joints across the full stride cycle for each running speed condition are presented in Figure 3. After an initial external rotation hip joint torque at foot strike, an internal rotation torque developed during initial stance, whereas an external rotation torque developed during terminal stance. The transverse-plane torque at the hip joint then fluctuated during initial and midswing before an external rotation torque developed during terminal swing. At the knee joint, an external rotation torque developed during stance, especially for faster running speeds. A degree of variability across participants was evident for the slower running speeds. At the ankle joint, an external rotation torque developed during stance. The peak magnitudes of the transverse-plane torques during stance displayed a significant speed effect at the hip and knee joints but not at the ankle (Table 1). Peak hip internal rotation torque during stance and peak knee external rotation torque during stance increased in absolute magnitude by 0.5 $N \cdot m \cdot kg^{-1}$ (2.02-fold) and 0.23 $N \cdot m \cdot kg^{-1}$ (2.15-fold), respectively, when running speed changed from 3.50 to 8.95 $m \cdot s^{-1}$.

The normalized mean ± SD net powers developed about the hip, knee, and ankle joints across the full stride cycle for each running speed condition are presented in Figure 4. At the hip, small bursts of power generation tended to occur during the first half of stance, especially at faster running speeds. From midstance onward, continuous phases in the hip joint power profile were clearly identifiable. Power was absorbed during terminal stance, generated during initial swing, then absorbed again during midswing, and finally generated during terminal swing. At the knee, power was absorbed during the first half of stance and generated during the latter half of stance. Power was also absorbed during terminal stance, generated during initial swing,. At the ankle, power was absorbed during the first half of stance and then generated for the remainder of stance. All 10 variables extracted from the lower limb joint powers displayed a significant speed effect (Table 1). However, a significant increase in absolute magnitude for all running speed increments was only demonstrated by four variables: peak hip joint power generation during initial swing, peak hip joint power generation during terminal swing, peak knee joint power absorption during initial swing, and peak knee joint power absorption during terminal swing. When running speed

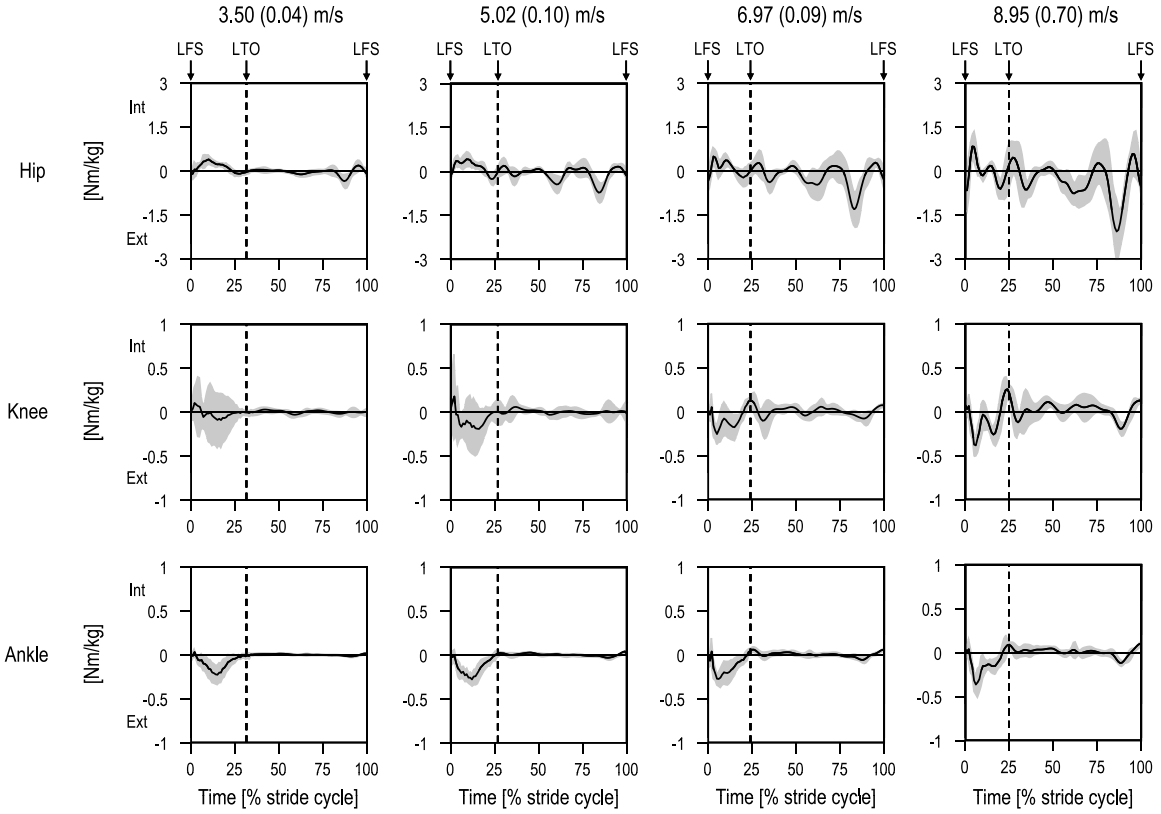

FIGURE 3—Transverse-plane torques developed about the hip (*top panels*), knee (*middle panels*), and ankle (*bottom panels*) joints across the full stride cycle for the left lower limb (left foot strike to left foot strike) for the four discrete running speeds. Data represent the group mean (*solid black line*) ± one SD (*gray shading*). The *dashed vertical line* indicates the average time (% stride cycle) of toe-off for each speed condition. LFS: left foot-strike; LTO: left toe-off; Ext, external rotation; Int, internal rotation.

changed from 3.50 to 8.95 $m \cdot s^{-1}$, these variables increased in absolute magnitude by 25.21 $W \cdot kg^{-1}$ (7.63-fold), 37.66 $W \cdot kg^{-1}$ (12.08-fold), 12.28 $W \cdot kg^{-1}$ (8.35-fold), and 32.54 $W \cdot kg^{-1}$ (8.06-fold), respectively.

Data for the amount of work done at the lower limb joints are contained in Table 1. The hip and ankle were found to be predominantly energy generators because the amount of positive work done over the stride cycle exceeded the amount of negative work done. Conversely, the knee joint was predominantly an energy absorber. The work done at the hip increased significantly with faster running. For example, the largest absolute change occurred during terminal swing, where the amount of positive work increased by 1.97 $J \cdot kg^{-1}$ (7.35-fold) when running speed changed from 3.50 to 8.95 $m \cdot s^{-1}$. At the knee, the total work done during stance was relatively invariant across running speed conditions, whereas the negative work done during initial swing and terminal swing increased in absolute magnitude by 1.02 $J \cdot kg^{-1}$ (6.37-fold) and 1.66 $J \cdot kg^{-1}$ (5.05-fold), respectively, when running speed changed from 3.50 to 8.95 $m \cdot s^{-1}$. At the ankle, the total work done during stance increased by 0.53 $J \cdot kg^{-1}$ (1.36-fold) from 3.50 to 5.02 $m \cdot s^{-1}$, but then increased by only 0.28 $J \cdot kg^{-1}$ (1.14-fold) thereafter.

When second-order polynomial trend lines were fitted to the data for each of the work variables, very little association was found between running speed and the work done at the knee joint during initial stance (work = $0.019 \times \text{speed}^2 - 0.223 \times \text{speed} - 0.179$; $R^2 = 0.10$) and terminal stance (work = $-0.002 \times \text{speed}^2 + 0.012 \times \text{speed} + 0.403$; $R^2 = 0.04$). Moderate associations occurred between running speed and the work done at the hip joint during terminal stance (work = $-0.007 \times \text{speed}^2 - 0.014 \times \text{speed} - 0.023$; $R^2 = 0.56$) and midswing (work = $-0.031 \times \text{speed}^2 + 0.249 \times \text{speed} - 0.605$; $R^2 = 0.74$) as well as at the ankle joint during initial stance (work = $0.013 \times \text{speed}^2 - 0.238 \times \text{speed} + 0.197$; $R^2 = 0.44$) and terminal stance (work = $-0.017 \times \text{speed}^2 + 0.288 \times \text{speed} + 0.220$; $R^2 = 0.50$). The strongest associations with running speed were found for the positive work done at the hip during initial swing ($R^2 = 0.83$) and terminal swing ($R^2 = 0.87$) and for the negative work done at the knee during initial swing ($R^2 = 0.89$) and terminal swing ($R^2 = 0.94$; Fig. 5).

DISCUSSION

The purpose of the current study was to evaluate the effect of running speed on lower limb joint kinetics to determine which biomechanical variables were most influenced by speed approaching maximal sprinting. Kinematic and ground reaction force data were collected from eight participants while running at four discrete speeds: 3.50 ± 0.04 $m \cdot s^{-1}$, 5.02 ± 0.10 $m \cdot s^{-1}$, 6.97 ± 0.09 $m \cdot s^{-1}$, and

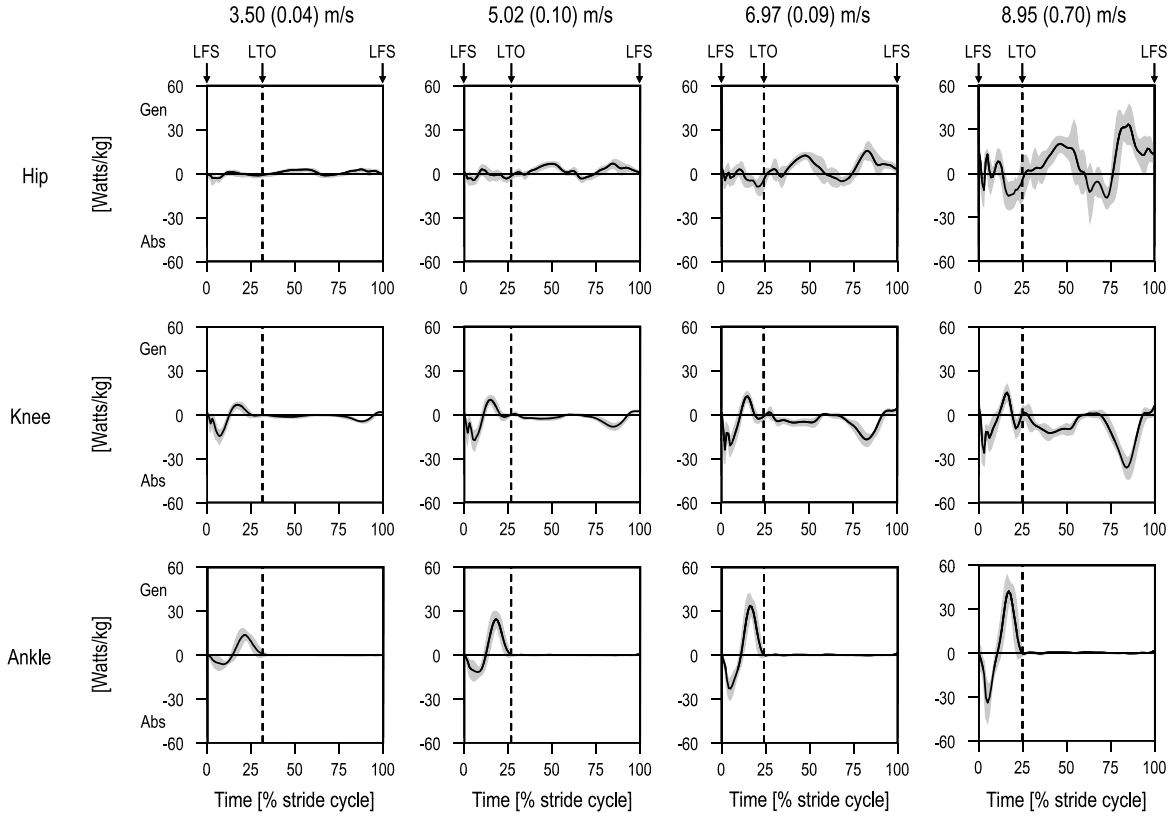

FIGURE 4—Net powers developed about the hip (*top panels*), knee (*middle panels*), and ankle (*bottom panels*) joints across the full stride cycle for the left lower limb (left foot strike to left foot strike) for the four discrete running speeds. Data represent the group mean (*solid black line*) ± one SD (*gray shading*). The *dashed vertical line* indicates the average time (% stride cycle) of toe-off for each speed condition. LFS: left foot-strike; LTO: left toe-off; Abs, absorption; Gen, generation.

8.95 ± 0.70 $m \cdot s^{-1}$. A standard inverse-dynamics approach was used to compute the three-dimensional torques at the lower limb joints, from which net powers and work were also calculated. The torques developed about the hip, knee, and ankle joints during running displayed identifiable profiles in all three anatomical planes (Figs. 1–3). Several interesting findings were revealed from the data. First, the variables that displayed the largest increases in absolute magnitude with faster running were the sagittal-plane torques, net powers, and work done at the hip and knee joints during terminal swing (Table 1; Figs. 1, 4, and 5). Second, the peak extension torque and work done at the knee joint during stance were found to be unaffected by increasing running speed (Table 1). Third, whereas the work done at the ankle

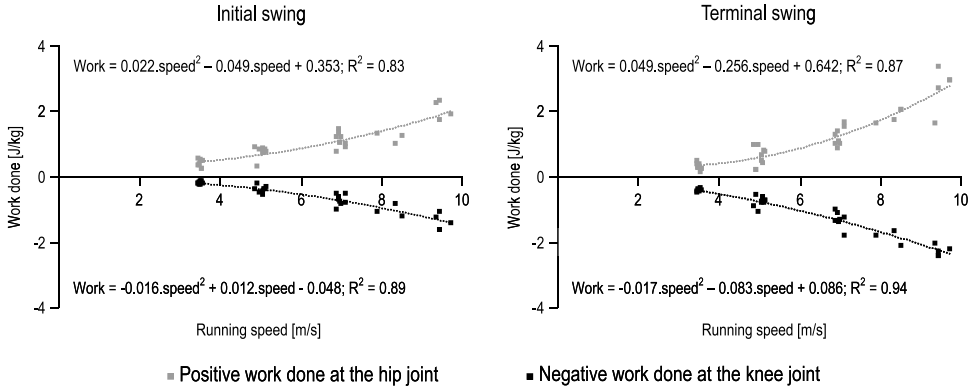

FIGURE 5—Work done at the hip and knee joints during initial swing (*left panel*) and terminal swing (*right panel*) with increasing running speed. The scatter plots contain data for each participant (*filled boxes*) for each speed condition as well as the second-order polynomial trend lines fitted to the data (*dotted lines*). Data for the positive work done at the hip joint are indicated in *gray*, whereas data for the negative work done at the knee joint are indicated in *black*. During initial swing, energy is generated at the hip joint primarily by the hip flexor muscles at the same time as energy is absorbed at the knee joint primarily by the knee extensor muscles. During terminal swing, energy is generated at the hip joint primarily by the hip extensor muscles at the same time as energy is absorbed at the knee joint primarily by the knee flexor muscles. Note that with increasing running speed, the gradient of the trend lines becomes steeper for the work done at the hip and knee joints during terminal swing when compared to initial swing.

joint during stance significantly increased when running speed changed from 3.50 to 5.02 $m \cdot s^{-1}$, it seemed to plateau when running speed progressed beyond 5.02 $m \cdot s^{-1}$ (Table 1). These results have important implications for lower limb muscle function with faster running. For example, when running speed progressed beyond 6.97 $m \cdot s^{-1}$, a substantial increase in biomechanical load occurred for the hip flexor and extensor muscles during swing compared with the knee extensor and ankle plantar–flexor muscles during stance. Furthermore, of all the major lower limb muscle groups, the hip extensor and knee flexor muscles during terminal swing demonstrated the most dramatic increase in biomechanical load with faster running.

There are several limitations associated with the methods used in the present study that need to be acknowledged. First, an inverse-dynamics approach was used to calculate lower limb joint torques during running. Although inverse dynamics as well as subsequent net power and work done calculations are well-accepted biomechanical analyses, such an approach is limited in its ability to provide quantitative information regarding muscle function, as a given torque can be produced by an infinite combination of muscle forces. Second, as skin markers were used to measure lower limb kinematics, it is likely that estimates of segment velocity and acceleration were associated with a degree of error due to soft tissue artifact, particularly for the thigh as running speed increased. Some of the large fluctuations in the computed hip joint torques during swing for the faster speeds of running may therefore be attributable to this error. To minimize soft tissue artifact as much as possible, two main strategies were taken: (a) thigh tracking markers were restricted to areas that have been shown to be associated with lesser amounts of soft tissue artifact, such as the anterolateral aspect of the distal third of the thigh (2,31); and (b) a hierarchical biomechanical model was used in this study, whereby the pelvic tracking markers were used to reconstruct the hip joint center and the shank tracking markers were used to reconstruct the knee joint center. The thigh tracking markers (which are likely prone to the largest amounts of soft tissue artifact) were therefore only used to reconstruct the additional anatomical location that was required, together with the hip and knee joint centers, to define the femoral anatomical coordinate system. Third, given the large amount of data collected and analyzed in this study, the sample size was restricted to eight participants. It is therefore possible that some of the variables that showed a significant effect for speed but did not display significant increases in absolute magnitude for all running speed increments on *post hoc* testing may have done so with a larger sample size (e.g., peak ankle joint power absorption and generation during stance). However, it is not expected that a larger sample size would alter the main conclusions from this study, which were also based on the evident associations between work done at the lower limb joints and running speed. Fourth, the sample analyzed in this study was somewhat heterogenous, composed of both male and female participants recruited from two alternative running-based sports. Finally, only a single trial was analyzed per speed condition for each participant. It is acknowledged that it would have been ideal to have analyzed several trials per speed condition for each participant. However, the criteria for a successful trial were that the participant achieved a running speed within 5% of the desired speed and also achieved a valid foot strike on a single force plate for the test leg. It often took several attempts to obtain a single successful trial for a given speed condition, especially for the faster speeds of running. Consequently, in an effort to collect all data within a reasonable time frame and avoid the potential confounding effect of fatigue, the study was limited to a single trial per speed condition for each participant.

When comparing data in the present study with that reported by previous researchers, there are many factors that must be taken into account. These factors include (i) running speeds tested; (ii) the particular region of the running task that has been evaluated, such as the acceleration versus steady-state speed regions; (iii) differences in the biomechanical model used, such as definitions of joint center locations; (iv) the sampling rate used to capture data; (v) the filtering technique applied to the data; (vi) the process used to normalize the data; and (vii) the reference frame used to express the components of the net torque vector at each of the joints, specifically, laboratory reference frame, proximal segment reference frame, distal segment reference frame, or nonorthogonal reference frame (i.e., joint coordinate system). Various combinations of these factors will explain any observed differences between the data from the current study compared with previous studies.

With the above factors in mind, data from the present study display reasonable quantitative consistency with previous data in the literature. Ae et al. (1) measured sagittal-plane torques and net powers at the lower limb joints across the full stride cycle from five skilled male sprinters running at 2.68, 3.89, 6.52, 7.86, and 9.59 $m \cdot s^{-1}$. Unfortunately, the study of Ae et al. (1) is only available in abstract format, and thus, very limited data are actually presented. Also, a two-dimensional approach was taken; thus, only sagittal-plane torques were evaluated. Despite these issues, data that are available in Ae et al. (1) are in agreement with the present study. For example, during terminal swing for sprinting at 9.59 $m \cdot s^{-1}$, Ae et al. (1) computed a peak hip extension torque of ~3.5 $N \cdot m \cdot kg^{-1}$, a peak knee flexion torque of ~2.0 $N \cdot m \cdot kg^{-1}$, and a peak knee power absorption of ~35.0 $W \cdot kg^{-1}$. These peak magnitudes are all quantitatively consistent with equivalent data from the current study (Table 1).

Other studies have reported sagittal-plane torques and net powers at the lower limb joints across a range of running speeds but have obtained data only for a certain phase of the stride cycle, specifically, either the stance (3,5) or the swing phase (33). In a study of 13 runners, Arampatzis et al. (3) reported peak stance knee extension torques ranging from 2.57 ± 0.46 to 2.98 ± 0.37 $N \cdot m \cdot kg^{-1}$ (1.16-fold increase) and peak stance ankle plantarflexion torques ranging from

2.79 ± 0.42 to 3.43 ± 0.49 N·m·kg^{-1} (1.23-fold increase) when running speed changed from 3.55 ± 0.19 to 6.59 ± 0.24 m·s^{-1}. These relative increases in magnitude were similar to the present study, where the peak stance knee extension and ankle plantarflexion torques increased by 1.15-fold and 1.36-fold, respectively, when running speed changed from 3.50 to 6.97 m·s^{-1} (Table 1). Belli et al. (5) measured sagittal-plane torques and net powers at the lower limb joints from nine middle-distance runners at running speeds of 4.0, 6.0, and 8.9 m·s^{-1}. When comparing results to the current study, one notable difference is that Belli et al. (5) found the peak stance knee extension torque to increase (1.57-fold) with faster running. This discrepancy might be explained by differences in running technique for middle-distance runners versus sprinters. Swanson and Caldwell (33) measured net powers during swing at the hip and knee joints for 12 male athletes while running on a level treadmill at 4.47 and 7.61 m·s^{-1}. Net powers from the current study for running speeds of 5.02 and 6.97 m·s^{-1} (Table 1) were between 1.5- and 3.3-fold greater than that reported by Swanson and Caldwell (33). It is possible that these differences are a consequence of contrasting experimental conditions: data from Swanson and Caldwell (33) were collected during treadmill running, whereas data from this study were obtained during overground running.

The profiles of the computed torques and net powers at the lower limb joints from this study also display good qualitative consistency with previous findings in the literature. With respect to the sagittal-plane torques, the profiles from the current study are near identical with those presented by Ae et al. (1), which, to our knowledge, is the only previous study to have presented torques at the hip, knee, and ankle joints across the full stride cycle for a range of running speeds. With respect to net powers, four distinct phases of power absorption and generation were identified in the current study at the hip joint (i.e., terminal stance power absorption, initial swing power generation, midswing power absorption, terminal swing power generation) and the knee joint (i.e., initial stance power absorption, terminal stance power generation, initial swing power absorption, terminal swing power absorption) (Fig. 4), which is consistent with previous studies (1,6,19,33,34,37). For the ankle joint, two distinct phases of power absorption and generation were identified in the current study (i.e., initial stance power absorption and terminal stance power generation) (Fig. 4), which is also in agreement with that from other studies (1,3,5,6,8,19,23,37). However, the profile of the hip joint power during initial stance is less consistent across the literature. In this study, a variable or burstlike pattern was found to exist, particularly for the faster speeds of running (Fig. 4). Whereas other researchers (1,6,19,37) have observed a similar profile to the current study, Belli et al. (5) found a distinct phase of continuous power generation at the hip during the initial stance.

Despite being a predominantly planar motion, this study demonstrated that the torques at the lower limb joints during running do contain appreciable three-dimensional components. Identifiable profiles were evident in all planes; however, some variability across participants was evident in the frontal- and transverse-plane torques developed about the knee joint (Figs. 2 and 3) during stance at the running speeds of 3.50 and 5.02 m·s^{-1}. This result suggests that participants displayed a degree of variability in the posture of their knee joint with respect to the ground reaction force in the frontal and transverse planes for the slower speeds of running. Although two previous studies also have reported three-dimensional torques at the lower limb joints during running (16,23), both were limited to stance phase data and a single speed of running only. Furthermore, Glitsch and Baumann (16) obtained data for a single subject only, whereas McClay and Manal (23) did not evaluate the hip joint. To our knowledge, no previous study has provided a complete description of the three-dimensional torques at the hip, knee, and ankle joints across a broad spectrum of running speeds. Data contained in Table 1 and Figures 1–3 are therefore important in terms of providing reference values for future studies to use for comparative purposes.

Of all the biomechanical variables evaluated in this study, the work done at the lower limb joints conveys the most critical information regarding muscle function (38). Positive work is work done during a concentric contraction, which represents a flow of energy from the muscles to the limbs (energy generation), whereas negative work is work done during an eccentric contraction, which represents a flow of energy from the limbs to the muscles (energy absorption). Given the significance of work done at the lower limb joints for understanding muscle function, the association between work and running speed was computed for all the periods in the stride cycle where it was evident that a continuous portion of positive or negative work was performed. A total of 10 periods were identified across all running speeds (Table 1; see Figure, Supplemental Digital Content 2, the 10 distinct periods of continuous positive or negative work done at the lower limb joints identified across the stride cycle for all running speeds, http://links.lww.com/MSS/A81). The strongest associations between work and running speed were found for the hip and knee joints during initial swing and terminal swing (Fig. 5). In contrast, the work done at the knee joint during stance was relatively invariant with running speed, whereas the work done at the ankle joint increased between 3.50 and 5.02 m·s^{-1} but then changed very little thereafter (Table 1). Such results are generally consistent with that previously reported in the literature by Ae et al. (1). Knowledge regarding the work done at the lower limb joints with faster running therefore has important implications for both swing and stance phase leg muscle function.

During the initial swing, the hip flexor muscles were found to generate energy at the same time as the knee extensor muscles absorbed energy, whereas during terminal swing the hip extensor muscles were found to generate energy at the same time as the knee flexor muscles absorbed

energy (Figs. 4 and 5). These findings provide insights into the function of the major biarticular muscles of the thigh, specifically, the rectus femoris and hamstring muscles (9). Such muscles have been proposed to act as "energy straps" by harnessing the energy from a moving body segment and transferring that energy to the next adjacent joint (24). Energy exchange via the rectus femoris may occur at two points in the stride cycle: (a) during terminal stance, where energy is absorbed at the hip and simultaneously generated at the knee; and (b) during initial swing, where energy is absorbed at the knee and simultaneously generated at the hip. However, the energy exchange occurring during initial swing is likely to be more critical, as it was found to have a far greater sensitivity to increasing running speed. During terminal stance, the energy absorbed at the hip displayed only a moderate association with running speed ($R^2 = 0.56$), whereas the energy generated at the knee displayed no association with running speed ($R^2 = 0.04$). Energy exchange via the hamstring muscles may occur during terminal swing, where energy is absorbed at the knee and simultaneously generated at the hip. On the basis of these results, it is speculated that, as running speed is progressed toward maximal sprinting, a dramatic increase in biomechanical load is likely imparted onto the rectus femoris and hamstring muscles during initial swing and terminal swing, respectively. It has been well documented that rectus femoris and hamstring muscle strain injuries are common in sports that involve repetitive bouts of sprinting, such as Australian Rules football (25) and soccer (4,14). The sensitivity of the work done at the hip and knee joints during initial swing and terminal swing to increasing running speed may potentially offer a biomechanical explanation for these clinical observations. Future studies using computer-based musculoskeletal modeling techniques to quantify the function of individual muscles with increasing speeds of running are needed to further explore these hypotheses.

In contrast to swing, it seems that the work done by the leg extensor muscles during stance changes very little when running speed is progressed beyond 5.02 $m \cdot s^{-1}$. Although the positive work done at the hip joint by the extensor muscles during early stance was not quantified, it is not anticipated that doing so would change this general conclusion. Such results can be used to identify the mechanisms by which humans run faster. There are two basic ways to increase running speed: one can push on the ground harder (i.e., increase stride length) and/or one can push on the ground more frequently (i.e., increase stride frequency). Data from the present study indicate that, to achieve speeds above 5.02 $m \cdot s^{-1}$, runners become increasingly reliant on more frequent ground contacts of similar force rather than more forceful ground contacts. However, it is important to note that this observation cannot be used to make definitive conclusions regarding the biomechanical limitation to maximal sprinting. On the basis of the experimental data reported by Weyand et al. (35,36), the ultimate limit to maximal sprinting would seem to be related to how hard and quickly a runner can push on the ground. More specifically, these researchers found that top speed was obtained when the impulse responsible for elevating the body against gravity (force applied normal to the ground multiplied by stance time) reduced to the minimum levels necessary to provide enough time to swing the leg into position for the next step (36). As running speed increases, stance time eventually becomes too short to allow the forces developed by the leg extensor muscles to reach their contractile maximums (35).

In summary, this study measured three-dimensional torques, net powers, and work done at the lower limb joints across a broad spectrum of running speeds. The results provide insights into the underlying biomechanical causes of the observed movement patterns at the hip, knee, and ankle joints during running. Of all the major lower limb muscle groups, the hip extensor and knee flexor muscles during terminal swing demonstrated the most dramatic increase in biomechanical load when running speed progressed toward maximal sprinting.

Funding for this project was provided by the Physiotherapy Research Foundation Tagged Sports Physiotherapy Australia Research Grant (T08-THE/SPA(1)018), an Australian Research Council Discovery Grant (DP0772838), and a VESKI Innovation Fellowship.

The authors have no conflicts of interest.

The results of the present study do not constitute endorsement by the American College of Sports Medicine.

REFERENCES

1. Ae M, Miyashita K, Yokoi T, Hashihara Y. Mechanical power and work done by the muscles of the lower limb during running at different speeds. In: Jonsson B, editor. *Biomechanics X-B*. Champaign (IL): Human Kinetics; 1987. p. 895–9.
2. Akbarshahi M, Schache AG, Fernandez JW, Baker R, Banks S, Pandy MG. Non-invasive assessment of soft-tissue artifact and its effect on knee joint kinematics during functional activity. *J Biomech*. 2010;43:1292–301.
3. Arampatzis A, Bruggemann GP, Metzler V. The effect of running speed on leg stiffness and joint kinetics in human running. *J Biomech*. 1999;32:1349–53.
4. Arnason A, Gudmundsson A, Dahl HA, Johannsson E. Soccer injuries in Iceland. *Scand J Med Sci Sports*. 1996;6:40–5.
5. Belli A, Kyrolainen H, Komi PV. Moment and power of lower limb joints in running. *Int J Sports Med*. 2002;23:136–41.
6. Bezodis IN, Kerwin DG, Salo AIT. Lower-limb mechanics during the support phase of maximum-velocity sprint running. *Med Sci Sports Exerc*. 2008;40(4):707–15.
7. Biewener AA, Farley CT, Roberts TJ, Temaner M. Muscle mechanical advantage of human walking and running: implications for energy cost. *J Appl Phsiol*. 2004;97:2266–74.
8. Buczek FL, Cavanagh PR. Stance phase knee and ankle kinematics and kinetics during level and downhill running. *Med Sci Sports Exerc*. 1990;22(5):669–77.
9. Chapman AE, Caldwell GE. Factors determining changes in lower limb energy during swing in treadmill running. *J Biomech*. 1983;16:69–77.
10. de Leva P. Adjustments to Zatsiorsky–Seluyanov's segment inertia parameters. *J Biomech*. 1996;29:1223–30.
11. Delp SL, Hess WE, Hungerford DS, Jones LC. Variation of

rotation moment arms with hip flexion. *J Biomech*. 1999;32: 493–501.
12. DeVita P, Skelly WA. Intrasubject variability of lower extremity joint moments of force during the stance phase of running. *Hum Mov Sci*. 1990;9:99–115.
13. Dillman CJ. A kinetic analysis of the recovery leg during sprint running. In: Cooper JM, editor. *Selected Topics on Biomechanics: Proceedings of the C. I. C. Symposium on Biomechanics, Indiana University, 1970*. Chicago (IL): Athletic Institute; 1971. p. 137–65.
14. Ekstrand J, Hagglund M, Walden M. Injury incidence and injury patterns in professional football: the UEFA injury study. *Br J Sports Med*. 2011;45(7):553–8.
15. El-Masri MM, Fox-Wasylyshyn SM. Missing data: an introductory conceptual overview for the novice researcher. *Can J Nurs Res*. 2005;37:156–71.
16. Glitsch U, Baumann W. The three-dimensional determination of internal loads in the lower extremity. *J Biomech*. 1997;30: 1123–31.
17. Harrington ME, Zavatsky AB, Lawson SE, Yuan Z, Theologis TN. Prediction of the hip joint centre in adults, children, and patients with cerebral palsy based on magnetic resonance imaging. *J Biomech*. 2007;40:595–602.
18. Hunter BV, Thelen DG, Hhaher YY. A three-dimensional biomechanical evaluation of quadriceps and hamstrings muscle function using electrical stimulation. *IEEE Trans Neural Syst Rehabil Eng*. 2009;17:167–75.
19. Johnson MD, Buckley JG. Muscle power patterns in the mid-acceleration phase of sprinting. *J Sports Sci*. 2001;19:263–72.
20. Kuitunen S, Komi PV, Kyrolainen H. Knee and ankle stiffness in sprint running. *Med Sci Sports Exerc*. 2002;34(1):166–73.
21. Mann R, Sprague P. A kinetic analysis of the ground leg during sprint running. *Res Q Exercise Sport*. 1980;51:334–48.
22. Mann RV. A kinetic analysis of sprinting. *Med Sci Sports Exerc*. 1981;13(5):325–8.
23. McClay I, Manal K. Three-dimensional kinetic analysis of running: significance of secondary planes of motion. *Med Sci Sports Exerc*. 1999;31(11):1629–37.
24. Novacheck TF. The biomechanics of running. *Gait Posture*. 1998; 7:77–95.
25. Orchard JW. Intrinsic and extrinsic risk factors for muscle strains in Australian football. *Am J Sports Med*. 2001;29:300–3.
26. Pandy MG, Lin Y-C, Kim HJ. Muscle coordination of mediolateral balance in normal walking. *J Biomech*. 2010;43:2055–64.
27. Schache AG, Baker R. On the expression of joint moments during gait. *Gait Posture*. 2007;25:440–52.
28. Schache AG, Baker R, Lamoreux LW. Defining the knee joint flexion-extension axis for purposes of quantitative gait analysis: an evaluation of methods. *Gait Posture*. 2006;24:100–9.
29. Simonsen EB, Thomsen L, Klausen K. Activity of mono- and biarticular leg muscles during sprint running. *Eur J Appl Physiol Occup Physiol*. 1985;54:524–32.
30. Simpson KJ, Bates BT. The effects of running speed on lower extremity joint moments generated during the support phase. *Int J Sport Biomech*. 1990;6:309–24.
31. Stagni R, Fantozzi S, Cappello A, Leardini A. Quantification of soft tissue artefact in motion analysis by combining 3D fluoroscopy and stereophotogrammetry: a study on two subjects. *Clin Biomech*. 2005;20:320–9.
32. Stefanyshyn DJ, Stergiou P, Lun VM, Meeuwisse WH, Worobets JT. Knee angular impulse as a predictor of patellofemoral pain in runners. *Am J Sports Med*. 2006;34:1844–51.
33. Swanson SC, Caldwell GE. An integrated biomechanical analysis of high speed incline and level treadmill running. *Med Sci Sports Exerc*. 2000;32(6):1146–55.
34. Vardaxis V, Hoshizaki TB. Power patterns of the leg during the recovery phase of the sprinting stride for advanced and intermediate sprinters. *Int J Sport Biomech*. 1989;5:332–49.
35. Weyand PG, Sandell RF, Prime DNL, Bundle MW. The biological limits to running speed are imposed from the ground up. *J Appl Physiol*. 2010;108:950–61.
36. Weyand PG, Sternlight DB, Bellizzi MJ, Wright S. Faster top running speeds are achieved with greater ground forces not more rapid leg movements. *J Appl Physiol*. 2000;89:1991–9.
37. Winter DA. Moments of force and mechanical power in jogging. *J Biomech*. 1983;16:91–7.
38. Winter DA. *Biomechanics and Motor Control of Human Movement*. New York (NY): John Wiley & Sons, Inc.; 2009. p. 370.
39. Woltring HJ. A Fortran package for generalised, cross-validatory spline smoothing and differentiation. *Adv Eng Software*. 1986;8: 104–7.
40. Yokozawa T, Fujii N, Ae M. Muscle activities of the lower limb during level and uphill running. *J Biomech*. 2007;40:3467–75.